의공학회지 : 제17권, 제4호, 1996
J. of KOSOMBE : Vol. 17, No. 4

연 구 논 문
96-17-4-13

SSFPI 기법을 이용한 MR 뇌기능 영상 -고속의 자화율 효과의 직접적인 측정

정순철·정준영·노용만*·조장희

= Abstract =

SSFP Interferometry (SSFPI) Technique Applied to functional MRI -A Fast and Direct Measurement of Magnetic Susceptibility Effect

S.C. Chung, J.Y. Chung, Y.M. Ro*, Z.H. Cho

We have developed a fast steady state free precession interferometry (SSFPI) technique which is useful for the fMRI (functional Magnetic Resonance Imaging). As is known, SSFP sequence with a suitable adjustment of gradient (readout) allows us to measure precession angle θ which in turn relates to the field inhomogeneity. Combining the two pulses (known as FID and Echo) in FADE (Fast Acquisition Double Echo) sequence, for example, one can obtain the interference term which is directly related to the precession angle θ. It has been known that a fast high resolution magnetic field mapping is possible by use of the modified FADE sequence or SSFPI, and we have attempted to use the SSFPI technique for the susceptibility-induced fMRI. When the method is applied to the susceptibility effect based functional magnetic resonance imaging (fMRI), it was found that the direct susceptibility effect measurement was possible without perturbations such as the backgrounds and inflow effect. In this paper, simulation results and experimental results obtained with 2.0 Tesla MRI system are presented.

Key words : fMRI, SSFPI, Field Mapping, Susceptibility Effect

INTRODUCTION

The field inhomogeneities encountered in MRI can be largely categorized by two; one caused by the magnet geometry and built-in inhomogeneity of the magnet, and the other inhomogeneity induced by the chemical shift and local susceptibility effect due to the paramagnetic substances inside the object. The former is measurable and can be corrected. The latter, however, is object dependent and cannot be measured. Especially the induced field inhomogeneity due to the susceptibility effect inside the object has been often a nuisance[1,2].

In the past, however, SSFP fast NMR imaging techniques have been used for fast field inhomogeneity measurement[3-5]. Notably the fast SSFP imaging technique has been used for rapid field inhomogeneity mapping using the interference principles of multi echo or double echo signals[6-9]. Advantage of the method is that, the method offers substantially shorter scan time than those of the other field mapping techniques and can easily be adopted in the conventional gradient echo or SSFP techniques.

한국과학기술원 정보및 통신공학과
Department of Information and Communication, KAIST, Seoul
* 대전대학교 컴퓨터공학과
* Department of Computer Engineering, Taejon University, Taejon
통신저자 : 정순철, (130-010) 서울시 동대문구 청량리동 207-43번지 한국과학기술원 정보 및 통신공학과
Tel. 958-3352, Fax. 965-4394
*본 논문은 1996년도 과학재단의 공모과제 연구비에 의하여 연구되었음

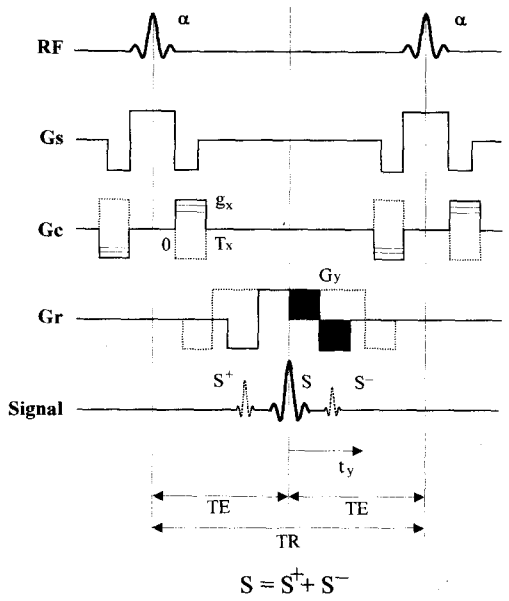

Fig. 1. Basic SSFPI (Steady State Free Precession Interferometry) sequence. This modified SSFP fast gradient echo imaging pulse sequence offers a simple and fast field inhomogeneity mapping. By suitable adjustments of the reading gradient, a interference pattern of the FID and echo signals can be obtained, i.e., adjusting the shaded areas, a and b, to an equal size. This interferogram will represent the field inhomogeneity. Note also that the sum of selection, coding and reading gradients is all becomes zero within a given TR.

Recent developments of the dynamic functional studies based on the susceptibility effect appears an ideal application example of the SSFPI techniques since the method offers direct measurements capability of the local susceptibility or map. In addition the method could offer inflow-effect free susceptibility effect measurement[10]. Although we have obtained susceptibility affected signal changes by the Conventional Gradient Echo (CGE) technique with small flip angle and long echo time, the results so far obtained are relatively poor in signal-to-noise ratio and appear to be contaminated by the large fraction of inflow effect[10-13]. It is, therefore, difficult to distinguish at least in the gradient echo technique, the change of oxygen level alone from the inflow effect in both the capillaries and small veins.

In this paper, a modified SSFP sequence namely SSFPI (SSFP Interferometry) is applied to dynamic functional studies in an attempt to quantitatively observe susceptibility effect without interference from such as the inflow effect, and other background signals. To verify the usefulness of the method (SSFPI), result is compared with the CGE technique and Tailored RF Gradient Echo (TRFGE) technique, respectively for reference.

THEORY and METHOD

Steady State Free Precessing Interferometry (SSFPI)

Let us first briefly review the SSFP fast gradient echo imaging technique. In Fig. 1, a modified SSFP fast gradient echo imaging sequence of a double echo data acquisitions known as FADE (Fast Acquisition Double Echo) is shown. When the original FADE sequence is used for the imaging, it is well known that there is two NMR signals which are known as FID (S^+) and echo signals (S^-) and given by,

$$S^+(g_x, t_y) = \iint \left[S_x^+(x, y) + jS_y^+(x, y) \right] exp \left[-j\gamma \left(x g_x T_x + y G_y t_y \right) \right] dxdy$$

;FID signal (1)

$$S^-(g_x, t_y) = \iint \left[S_x^-(x, y) + jS_y^-(x, y) \right] exp \left[-j\gamma \left(x g_x T_x + y G_y t_y \right) \right] dxdy$$

;echo signal (2)

where S_x^+, S_x^-, S_y^+, and S_y^- are the x-and y-components of the transverse spin magnetizations before and after the application of RF pulse, respectively. For the sake of simplicity, T_2-decay processes during the echo time are omitted in Eq.s (1) and (2). When the time duration of reading gradient (shaded region) is adjusted and made equal, the FID and echo signals will be merged together and form a single nuclear signal which is believed to be an interference signal or an interferogram representing the field inhomogeneity,

$$S(g_x, t_y) = S^+(g_x, t_y) + S^-(g_x, t_y)$$

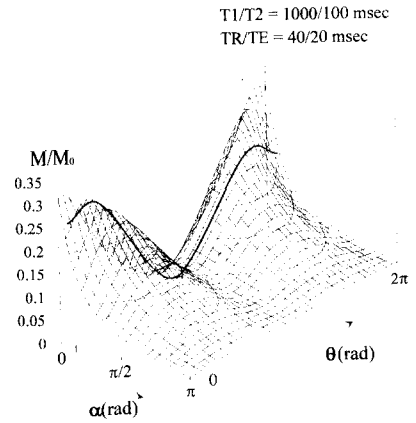

Fig. 2. (a) Normalized voxel signal intensities as a function of the free precession angle (0 to 2π) and the flip angle α(0 to π) for a given TR/TE=40/20(msec) with T1/T2 = 1000/100 (msec)

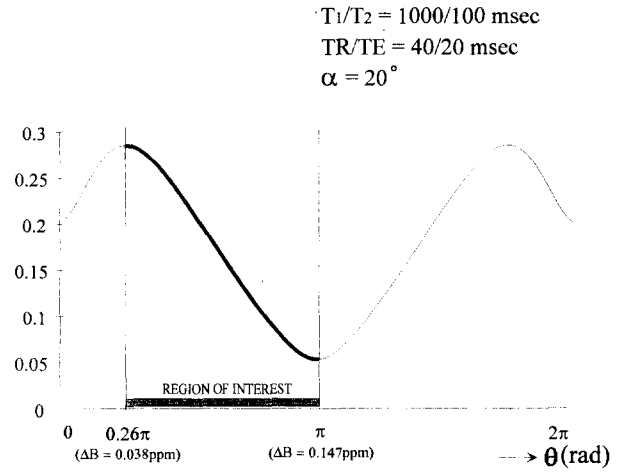

Fig. 2. (b) A same plot for a fixed α, i.e., $\alpha=20°$ with varying θ(0 to 2π). Normalized voxel signal intensities falling into the linear region: indicated with thick lines. By adjusting TR, range of the phase θ should be placed in the linear region shown

$$\iint\Big[\Big(M_x^{+}(x,\ y)+M_x^{-}(x,\ y)\Big) + j\Big(M_y^{+}(x,\ y)+M_y^{-}(x,\ y)\Big)\Big] \cdot exp\Big[-j\gamma\Big(xg_xT_x+yG_yt_y\Big)\Big]dxdy \tag{3}$$

where S, S^+, and S^- are illustrated in Fig. 1.

Fourier transformation of Eq. (3) results in an image signal which is given by,

$$M(x,y)=\frac{M_0\sin\alpha(1-E_1)\Big[4E_2^2\sin^2\theta+(1-E_2^2)^2\Big]^{1/2}}{(1-E_1\cos\alpha)(1-E_2\cos\theta)-(E_1-\cos\alpha)(E_2-\cos\theta)E_2} \tag{4}$$

where M_0, α, θ, E_1, and E_2 are the equilibrium spin magnetization, flip angle, free precession angle of the transverse spin magnetization during the pulse repetition interval TR, $E_1=\exp(-TR/T_1)$, and $E_2=\exp(-TR/T_2)$, respectively. It is interesting to observe that Eq. (4) is a function of the free precession angle θ, and in turn free precession angle θ is related to the field inhomogeneity provided that suitable values of the flip angle α, E_1 and E_2 are chosen. Since the free precession angle θ is the time integration of the magnetic fields existing in the given imaging situation, including the field inhomogeneity $\Delta B(x, y)$, θ can be written as,

$$\theta=\int_0^{TR}\gamma\Big[\Delta B(x,y)+xG_x(t)+yG_y(t)\Big]dt \tag{5}$$

where TR is the repetition time, $G_x(t)$ and $G_y(t)$ are the x- and y-directional gradient fields, respectively. For the fast SSFP gradient echo sequence shown in Fig. 1, $\int_0^{TR}G_x(t)dt$ and $\int_0^{TR}G_y(t)dt$ terms will cancel out, consequently Eq. (5) can simply be written as,

$$\theta=\int_0^{TR}\gamma\,\Delta B(x,y)\,dt=\gamma\,\Delta B(x,y)\,TR \tag{6}$$

Equation (4) and (6) suggest a possible measurement of the field inhomogeneity $\Delta B(x,y)$, i.e., Eq. (4) implies that the voxel signal intensity M(x,y) represents an interference pattern of the FID and echo signals hence the precession angle θ, i.e., signal intensity appears as a periodic function of field inhomogeneity. θ dependent signals are plotted in Fig. 2(a) for a period between 0-2π as a function of θ for different values of α. In Fig. 2(b), an example of signal amplitude variations as a function of θ for a given set of values T_1, T_2, TE and α, namely TR/TE=40/20(msec) and T_1/T_2=1000/100(msec) with a α of 20°. By suitable adjustment of TR, a linear relation between inhomogeneity strength (θ) and signal intensity (M/M_0) can be obtained. As shown in Fig 2(a), as α becomes smaller, the sensitivity of susceptibility

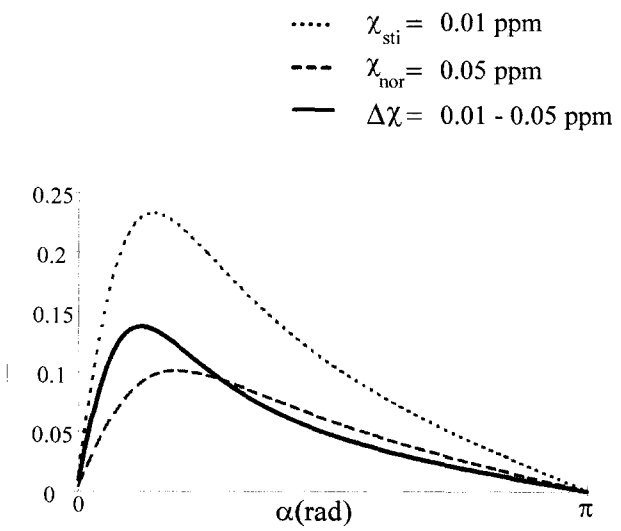

Fig. 3. Assuming that stimulation stage and normal stage produce susceptibility χ_{STI} =0.01ppm and χ_{NOR}=0.05ppm, respectively, normalized voxel signal intensities of each as a function of the flip angle α are plotted at SSFPI sequence together with the differences ($\Delta\chi=\chi_{STI}-\chi_{NOR}$). The latter is the signal to be used for fMRI

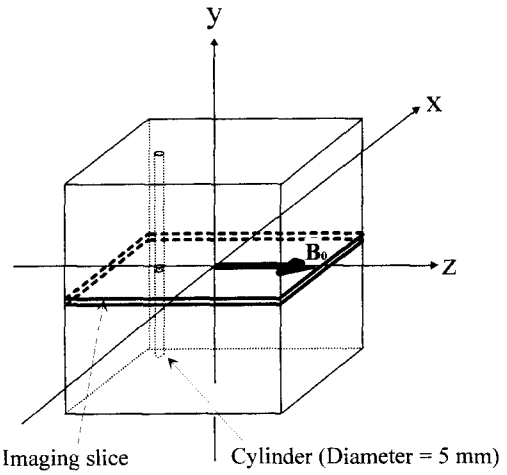

Interior susceptibility of the cylinder : χ_i
Exterior susceptibility of the cylinder : χ_e
Susceptibility difference : $\Delta\chi=\chi_e-\chi_i$

Fig. 4. A simple model used for the computer simulation. In this model, a cylindrical tube (representing the veins or a group of capillaries) of diameter D=5(mm) is placed in perpendicular to the B_0 field direction

difference, therefore, the signal to noise ratio becomes larger as the linear region increases. To observe the linear region in detail the signal variations are plotted in Fig. 2(b) for a fixed value of $\alpha=20°$ and observed signal intensity as a function of θ(0 to 2π). When θ varied one period, i.e., between 0 and 2π, the field inhomogeneity. ΔB varied from 0 ppm to 0.294 ppm for a given TR (~40 msec) with B_0 = 2 Tesla (see Eq. (6)). The linear region is thus variable as a function of, for example, TR. For this example a linear region selected is chosen between $\theta=0.26\pi$ and $\theta=\pi$. From Eq. (6), the field inhomogeneity ΔB that coincides with the above θ value are between 0.038ppm (at $\theta=0.26\pi$) and 0.147ppm (at $\theta=\pi$). By suitable adjustment of the TR, a linear relation between strength of the inhomogeneity and signal intensity can be obtained. Therefore, if a field inhomogeneity induced by susceptibility effect lies within the linear region (region of interest) of the curve, the susceptibility effect can be measured directly. When it is suitably adjusted and applied to the 2-dimensional imaging, it will provide an inhomogeneity map useful for the imaging of chemical shift and susceptibility effects. Since the chemical shift effect is negligible in brain imaging, the method offers fast and direct way of measuring the susceptibility effects in fMRI.

Susceptibility Effect in Blood

The volume susceptibility of whole deoxygenated blood was known to be 0.08ppm at 2 Tesla[14]. Using oxygenation of the hemoglobin, the magnetic susceptibility difference in blood can be written as;

$$\Delta\chi_{v.\,blood}(Y)=(1-Y)\,\Delta\chi_{v.\,blood}(Y=0) \tag{7}$$

where Y is the fraction of oxygenated hemoglobin. For human, the fraction of oxygenated hemoglobin Y can be calculated from the blood oxygenated curve which is given as[15]

$$\frac{Y}{1-Y}=\left[\frac{pO_2}{P_{50}}\right]^{2.8} \tag{8}$$

where pO_2 is the partial pressure of oxygen in the blood and P_{50} is the partial pressure of oxygen at which half of the hemoglobin sites are bound (P_{50} = 26 torr). Assuming partial oxygen pressure in capillaries varies between 20 and 40 torr where 20 torr corresponds to the normal stage while 40 torr corresponds to the stimulated or oxygen rich state, respectively[16]. Then the susceptibility differences are calculated assuming that the normal susceptibility,

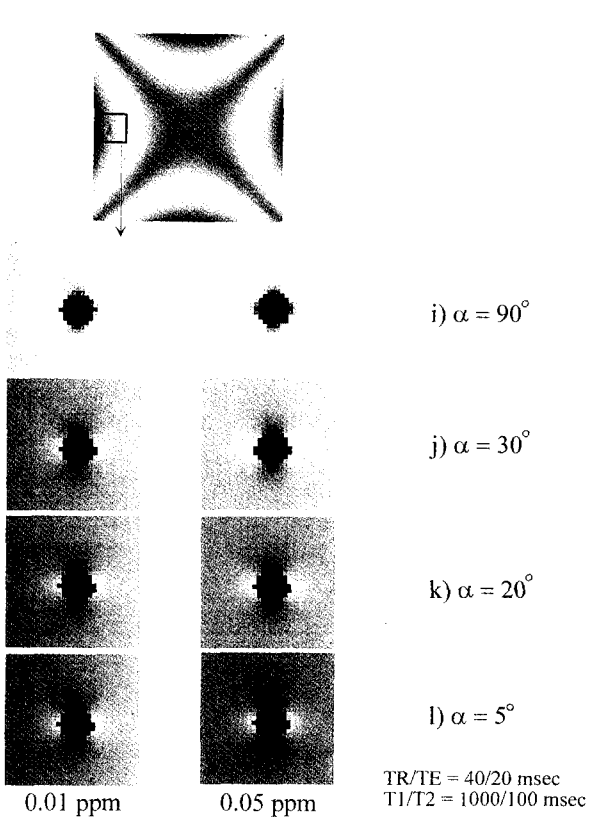

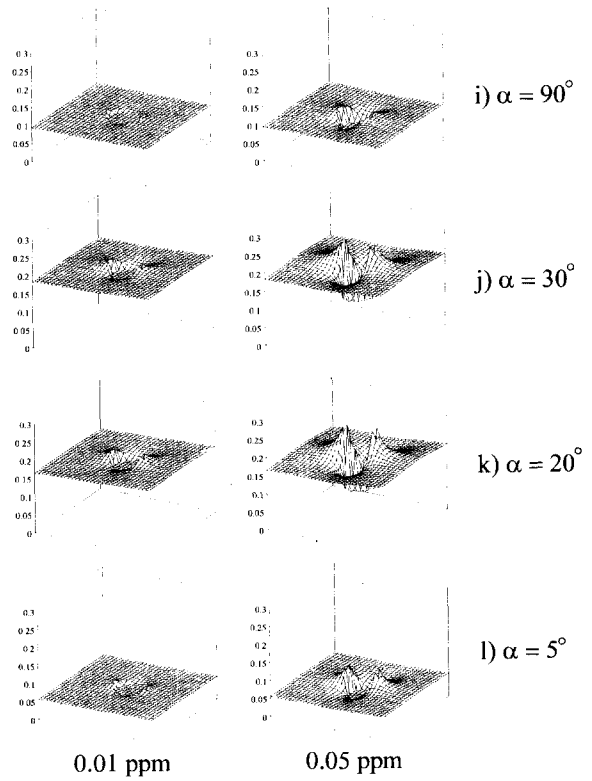

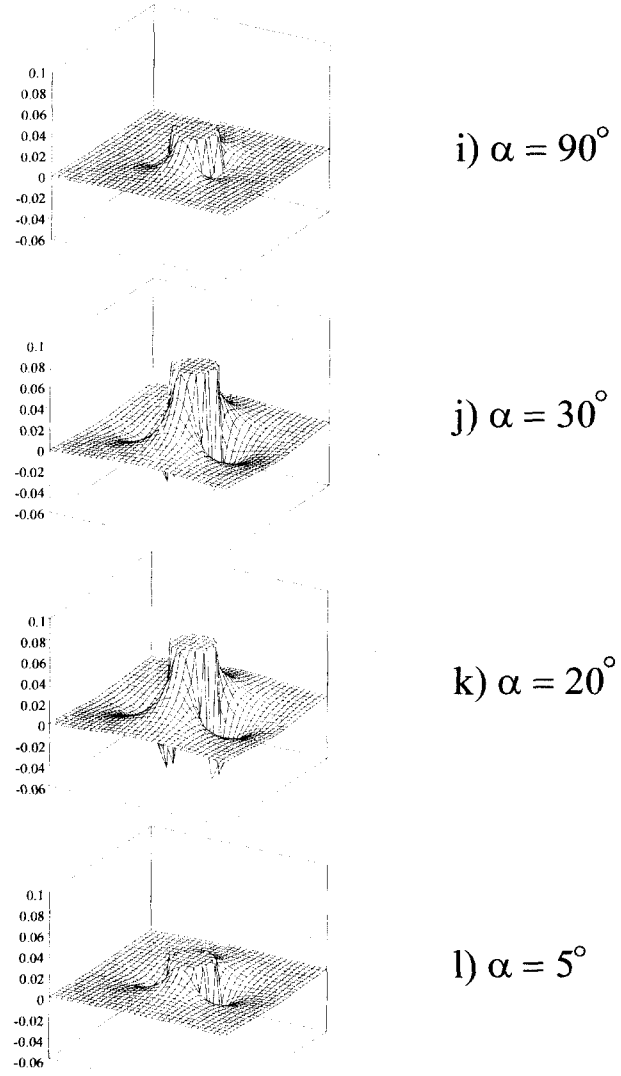

Fig. 5. (a) SSFPI gradient echo simulation results with varying flip angle from 5° to 90° with TR/TE=40/20 (msec) and T1/T2=1000/100(msec). Images at the left and right are the cases correspond to χ = 0.01ppm, 0.05ppm. (b) The corresponding perspectively views and (c) difference perspectively data

χ_{nor}, is about 0.05 ppm (pO_2 = 20 torr) at normal stage while χ_{sti} is about 0.01 ppm (pO_2 = 40 torr) at stimulation stage using Eq. (7) and (8). Assuming main magnetic field inhomogeneity (ΔB_0) is in the order of 0.04ppm in our imaging of interested region (visual cortex) and the susceptibility χ was calculated varying the flip angle α for the χ between the normal to the stimulation. The normalized magnetization versus flip angle α is calculated using Eq. (4) and plotted in Fig. 3. Since the ΔB_0 is assumed to be

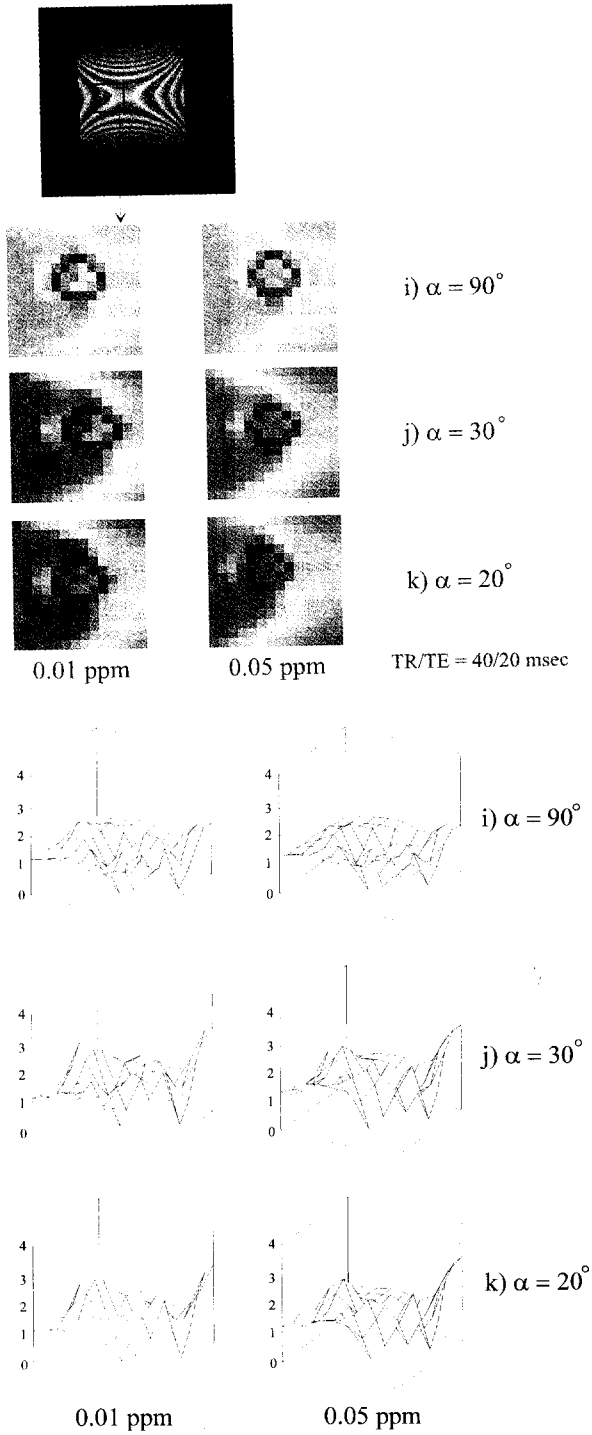

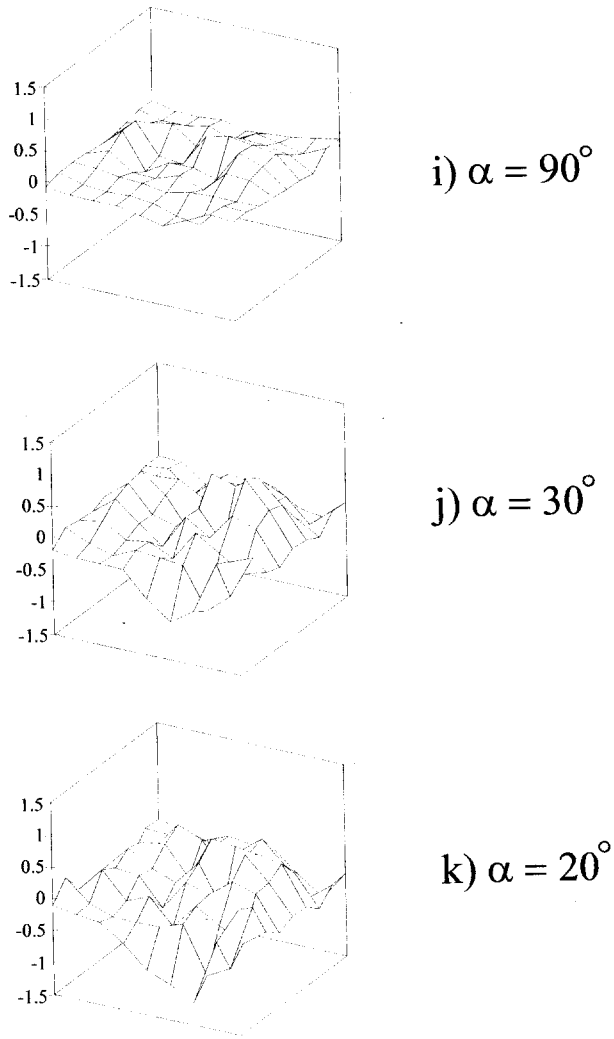

Fig. 6. An experimental phantom consisting of a tube with a different susceptibility value 0.11ppm $CuSO_4$ solution and 0.15ppm $CuSO_4$ solution immersed in water (0.1ppm $CuSO_4$ solution) as shown in Fig. 4, so that susceptibility difference is 0.01ppm and 0.05ppm, respectively. (**a**) SSFPI gradient echo experimental results with varying flip angle α from 20° to 90° with TR/TE=40/20 (msec). Images at the left and right are the cases correspond to χ = 0.01ppm, 0.05ppm. (**b**) The corresponding perspectively views and (**c**) difference perspectively data

0.04ppm, the range of total field inhomogeneity variations become roughly between 0.05ppm ($\Delta B_0 + \chi_{sti}$) and 0.09ppm ($\Delta B_0 + . \chi_{nor}$) and this range resides well within the linear region for the case of TR/TE= 40/20(msec) and T_1/T_2=1000/100(msec) shown in Fig. 2(b). As seen, in Fig. 3 the sensitivity of susceptibility difference ($\Delta\chi=\chi_{sti}-\chi_{nor}$) is maximum value at near the $=\alpha 15° \sim 30°$. This calculation assures us that sensitive detection of tissue oxygenation differences is possible when a suitable adjustment is made in SSFPI technique.

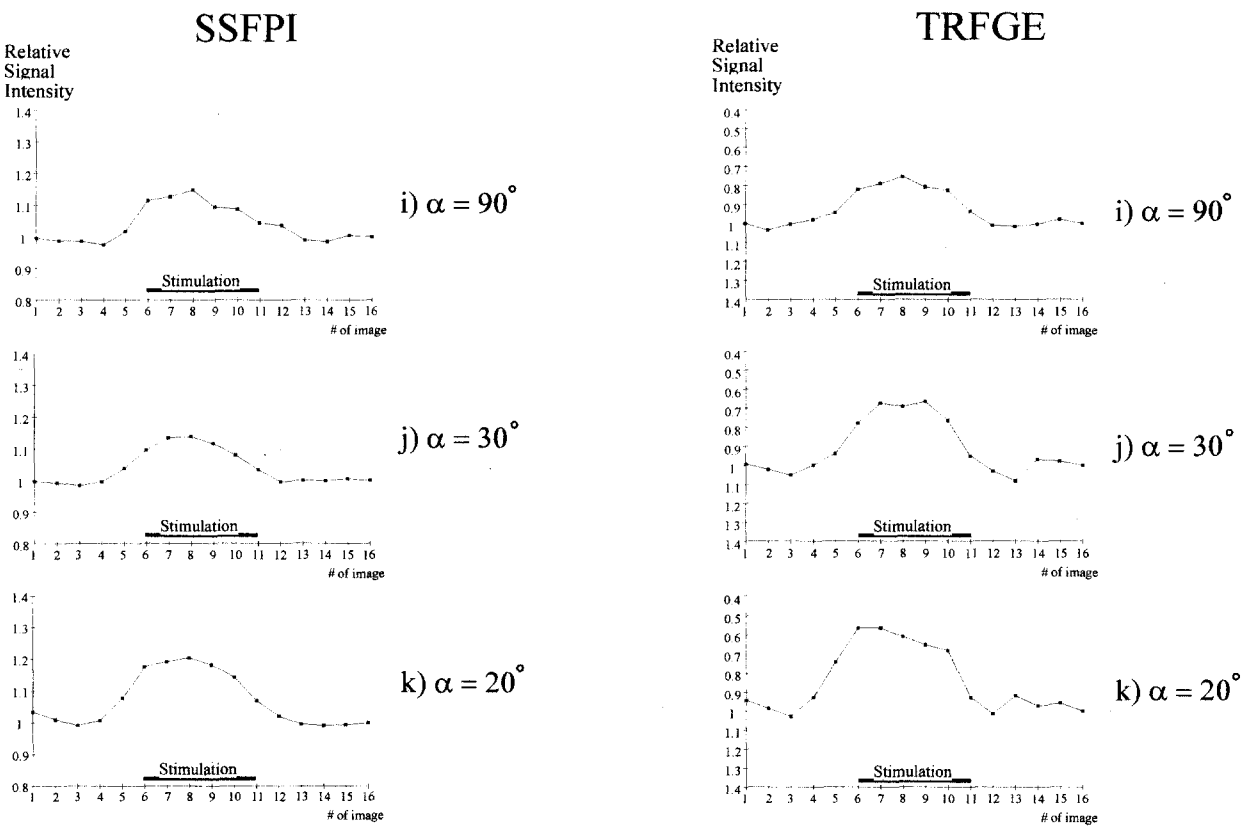

Fig. 7. The functional time course data obtained by 3 different methods, i.e., SSFPI, CGE, TRFGE near the visual cortex area. (a)The time course data were obtained for three different flip angles, 20°, 60°, and 90° with TR/TE =58/30(msec) by SSFPI sequence. (b) Same as (a) obtained by CGE sequence. (c) Same as (a) obtained by TRFGE sequence

Computer Simulation

For the imaging simulation, first the value of main magnetic field is calculated at each pixel and secondly a new main magnetic field value at each pixel affected by the susceptibility effect is calculated. The new interior magnetic field B_i and the value of external magnetic field $(B_e)_z$ and $(B_e)_x$ in the directions to z and x axes are calculated using the Eq. (9) and (10), respectively, and is given by[17]

$$B_i = B_{oi}\left[1 - \frac{\Delta\chi}{2}\right] \tag{9}$$

$$(B_e)_z = B_{oi}\left[1 - \frac{\Delta\chi}{2}\, R^2 \frac{z^2 - x^2}{r^4}\right] \tag{10}$$

$$(B_e)_x = -B_{oi}\frac{\Delta\chi}{2}\,R^2\frac{2\chi z}{r^4} \qquad (10b)$$

where B_{oi} is the value of the main magnetic field which we have assumed as total of 0.147ppm in both z- and x-directions as a function of $r(r=\sqrt{x^2+z^2})$ and $\Delta\chi = \chi_e - \chi_i$. Next, the new field inhomogeneity values (B_i, $(B_e)_z$, and $(B_e)_x$) are calculated using the Boi at each pixel and relative signal intensity (M/M_0) is calculated and then plotted.

For 2-D image simulation with SSFPI sequence, we consider a simple model, shown in Fig. 4(a), in which a 5mm diameter tube filled with agent (such as a group of capillaries) situated in perpendicular to B_0 direction. In Fig. 5(a) SSFPI gradient echo images (coronal views) are obtained and zoomed when χ is varied between 0.01ppm and 0.05ppm (assuming χ_{sti} = 0.01ppm, χ_{nor} = 0.05ppm) inside the tube and perspective view is also plotted in Fig. 5(b). It is also assumed that the total main magnetic field inhomogeneity in z-direction and x-direction varied total of 0.147ppm, i.e., θ varied about between 0 and π (1/2 periods) at each direction. The tube is located in the linear region, i.e., the tube is located between $\theta = 0.26\,\pi$ and π. In Fig. 5(a), flip angle α is varied from 5° to 90° and corresponding perspective view is plotted in Fig. 5(b). The distortion of field pattern appears in the area that where the tube is located, i.e., where susceptibility change occurred, signal intensity change is observed. By subtraction of χ_{nor} from χ_{sti} tissue oxygenation differences in the capillary can be inferred as shown in Fig. 5(c). The sensitivity of susceptibility difference is maximized at near the $\alpha = 15° \sim 30°$ which is in agreement with the calculation in Fig. 3.

EXPERIMENTAL RESULTS AND DISCUSSIONS

To experimentally demonstrate the validity of the proposed field inhomogeneity mapping technique, we have obtained phantom experimental results and displayed in Fig. 6. An experimental phantom consisting of a tube with a different susceptibility value 0.11ppm $CuSO_4$ solution and 0.15ppm $CuSO_4$ solution immersed in water (0.1ppm $CuSO_4$ solution) as shown in Fig. 4, so that susceptibility difference is 0.01ppm and 0.05ppm, respectively. Field inhomogeneity maps of a phantom is obtained using imaging parameters of TR/TE=40/20 (msec) with $\alpha = 20° \sim 90°$ and perspective view and difference data are also plotted in Fig. 6(b) and (c).

After the first experimental observation, we proceeded with functional imaging by photic stimulation using a head coil on 2.0T whole body MRI. To make a comparative examination, CGE, TRFGE, and SSFPI experiments were consecutively performed on a normal volunteer. For the fMRI, time course studies were performed by varying the flip angle from 20° to 90° with TR/TE=58/30(msec). A single oblique slice of 10(mm) thick was selected in parallel to the calcarine fissure. TR was so adjusted that the variation lies in the linear region for SSFPI fMRI (See Fig. 2). A set of 15 images were obtained with and without photic stimulation by each technique with a time interval 9 sec. The first 5 and last 5 images were obtained during rest period and images from 6 to 10 were obtained during the photic stimulation. Time course signal processing was carried out using the correlation coefficient (cc) for each pixel[18]. The box-car waveform was used as the reference waveform[18]. The value of cc always varies between +1 and -1. A threshold value TH was set between 0 and +1 and data in each pixel were selected based on

$$cc \geq TH. \qquad (11)$$

These data are then superimposed the images acquired during the rest period. Fig. 7(a) shows the results of SSFPI with TH=0.6 for flip angles of 20°, 60° and 90°, respectively with TR/TE = 58/30 (msec). Subsequent experiments with CGE and TRFGE are shown in Fig. 7(b) and (c), respectively [19].

It is interesting to note that the signal variations in the SSFPI show a maximum sensitivity at low flip angle, as expected, while with increased flip angle (60°) the sensitivity dropped appreciably. Further increase of the flip angle, sensitivity is increased again as it is observed. The latter can be interpreted as the consequence of the inflow effect with very large flip angle (90°). This is also consistent with the subsequent time course data obtained with CGE where in-

flow effect is again clearly seen as the flip angle increases (see Fig. 7(b)). As discussed in the previous paper by the present authors 19 , the inflow effect is seen in CGE but is not seen in TRFGE, as it is clearly demonstrated in Fig. 7(c). This inflow effect free susceptibility effect measurement is one of the important advantages of the SSFPI technique for fMRI application. Another advantage that can be mentioned and useful for applications is the fact that the SSFPI does not require tailored RF pulse, as in the case of TRFGE sequence, hence the implementation is simpler than the TRFGE sequence.

In conclusions, we have presented a new method of performing fMRI using a modified SSFP technique which provides field map or field interferogram, i.e., susceptibility field map which is dependent on the status of the oxygenation in the veins and capillaries. Proposed SSFPI technique, therefore, provides a simple means to susceptibility only fMRI free from the inflow effect which often obscure the real susceptibility measurement in fMRI.

REFERENCES

1. C.H.Durney, and C.C.Johnson, "*Introduction to Modern Electromagnetics*", McGraw-Hill, 179, 1969.
2. W.H.Hayt, "*Engineering Electromagnetics*", McGrow-Hill, 313, 1981.
3. S.Y.Lee and Z.H.Cho, "*Fast SSFP Gradient Echo Sequence for Simultaneous Acquisitions of FID and Echo Signals*", MRM 8:142-150, 1988.
4. D.J.Kim and Z.H.Cho, "*Analysis of the Higher-Order Echoes in SSFP*", MRM 19:20-30, 1991.
5. J.Henning, "*Generalized MR Interferography*", MRM 16:390-402, 1990.
6. R.C.Hawkes, and S.Patz, "*Rapid Fourier Imaging Using Steady State Free Precession*", Magn.Reson. Med., Vol.4, 9, 1987.
7. M.L.Gyngell, "*The Application of Steady-State Free Precession in Rapid 2DFT NMR Imaging: FAST and CE-FAST Sequences*", Magn.Reson.Med., Vol.6, 415, 1988.
8. T.W.Redpath, and R.A.Jones, "*FADE-A New Fast Imaging Sequence*", Magn.Reson.Med., Vol.6, 224, 1988.
9. K.Sekihara, "*Steady-State Magnetizations in Rapid NMR Imaging Using Small Flip Angles and Short Repetition Intervals*", IEEE Trans. on Med. Imaging, Vol.6, 157, 1987.
10. Z.H.Cho, Y.M.Ro, J.B.Park, S.C.Chung, S.H.Park, "*Functional brain imaging using blood flow changes*" in Proc., SMRM, 12th Annual Meeting, Vol.1, 170, 1993.
11. K.K.Kwong, J.W.Belliveau, D.A.Chesler, I.E.Goldberg, R.M.Weiskoff, B.P.Poncelet, D.N.Kennedy, B. E.Hoppel, M.S.Cohen, R.Turner, H.Cheng, T.J. Brady, B.R.Rosen, "*Dynamic magnetic resonance imaging of human brain activity during primary sensory stimulation*" Proc. Natl. Acad. Sci. (USA) 89, 5675-5679, 1992.
12. S.Ogawa, D.W.Tank, R.Menon, J.M.Ellerman, S. Kim, H.Merkle, K.Ugurbil, "*Intrinsic signal changes accompanying sensory stimulation: functional brain mapping using MRI*" Proc. Natl. Acad. Sci. (USA) 89, 5951-5955, 1992.
13. Z.H.Cho, Y.M.Ro, S.H.Park, S.C.Chung, R.Ong, " *NMR Functional Imaging Using Tailored RF Gradient Echo Sequence-A True Susceptibility Measurement Technique*", Proc, SMR, Second Meeting, Vol. 2, 659, 1994.
14. K.R.Thulborn, J.C.Waterton, Paul M. Mathews, George Radda, "*Oxygenation Dependence of the Transverse Relaxation Time of Water Protons in Whole Blood at High Field*", Biochim. Biophy. Acta. 714, 265-270, 1982.
15. L. Stryer, "*Biochemistry*", 2nd ed., W.H. Freman and Company, New York, 1981.
16. Richard P. Kennan, Jianhui Zhong, John C. Gore, "*Intravascular Susceptibility Contrast Mechanisms in Tissues*", MRM 31:9-21, 1994.
17. K.M.Ludeke, P.Roschmann and R. Tischler,"*Susceptibility Artefacts in NMR Imaging*", MRI 3: 329-343, 1985.
18. Peter A. Bandettini, A. Jesmanowicz, Eric C. Wong, James S. Hyde, "*Processing Strategies for Time-Course Data Sets in Functional MRI of the Human Brain*", MRM 30:161-173, 1993.
19. Z.H.Cho, Y.M.Ro, S.H.Park, and S.C.Chung, "*NMR Functional Imaging Using Tailored RF Gradient Echo Sequence-A True Susceptibility Measurement Technique*", MRM 35:1-5, 1995.

=국문초록=

본 논문에서는 뇌기능 영상에 유용한 정상상태 자유세차 간섭기법 (SSFPI) 을 연구하였다. FADE (Fast Acqusition Double Echo) 기법에서의 두 가지 신호 (FID and Echo)를 결합하면 세차 각도 θ에 직접 관여하는 간섭무늬를 얻을수 있다. 즉, FADE를 변조한 SSFPI기법을 이용하면 고속, 고정밀의 자계 지도를 얻을 수 있는데 이것을 뇌기능 영상의 자화율 측정에 이용하는 것이다. 이 기법을 자화율 효과에 기본을 둔 뇌기능 영상에 적용했는데, 직접적인 자화율 효과를 측정할 수 있음을 컴퓨터 모의 실험과 실제 실험을 통해 증명할 수 있었다. 또한 이 기법은 잡음이나 혈류 효과와 같은 뇌기능 영상에서 실제 신호 (자화율 효과)에 영향을 미치는 간섭 신호를 제거할 수 있는 잇점도 있었다.